RSC Advances

PAPER

View Article Online
View Journal | View Issue

Cite this: *RSC Adv.*, 2020, **10**, 32265

Research and application of a high-performance fluorocarbon plate prepared *via* modified a high temperature mould pressing method

Pan Zhang,[ab] Ye Wang,[ab] Yi-rui Shu,[ab] Yan-jun Zhong,[ab] Wei Wang[ab] and Lin Yang *[ab]

Received 17th July 2020
Accepted 10th August 2020

DOI: 10.1039/d0ra06203k

rsc.li/rsc-advances

As an indispensable part of the production of electrolytic fluorine, the quality of the carbon plate determines the running conditions and technical and economic indexes of electrolytic cells. Therefore, improving the service life of carbon plates has become an urgent challenge. Herein, special fluorocarbon plates were successfully prepared *via* direct heating and asphalt impregnation based on the resistance of the carbon plates, which not only improved their performance index, but also greatly reduced the cost of their production. According to electron microscopy (SEM) observation, the carbon plate prepared by the hot pressing method possessed a more compact internal structure and dislocation phenomenon, which reduced the contact pores between particles, increased the density and reduced the resistivity. The prepared carbon plate exhibited a density of 1.81 g cm^{-3}, resistivity of 25.8 μΩ m, and service life of 151 days. These results are superior to that of industrial carbon plates with a density of 1.74 g m^{-3}, resistivity of 36.7 μΩ m, and run time of 90 days, where our fabricated carbon plate exhibited an improvement of 4.5%, 29.7%, and 67.7%, respectively.

1 Introduction

In the modern era, electrolysis is still the only way to produce industrial fluorine.[1] With the discovery of nuclear fission and its military and civilian effects, fluorine gas developed rapidly. Fluorine gas is widely used in electronics, laser technology, medicine, plastics, petrochemicals, aerospace and other fields. As an important material in the preparation of fluorine, the properties of the carbon anode directly affect the process and cost to produce electrolytic fluorine. In recent years, with the increasing demand for UF_6 products in China, the amount of carbon positive plates used for uranium conversion production has increased by 300%.[2] In the process of fluorine production, 10% of electrolytic cells cannot work normally every month due to the polarization, fracture and replacement of the carbon plates.[3,4] Therefore, improving the performance of the carbon positive plates to reduce their polarization, damage, and replacement frequency has become an urgent task in industry.

For more than two hundred years, the production of electrolytic fluorine has been developed using nickel, graphite and amorphous carbon. Nickel has high electrical conductivity and produces anodic polarization even if the electrolyte has a high water content.[5] However, nickel is not suitable for the mass production of fluorine gas due to its metal properties and short electrochemical corrosion life. Graphite electrodes are easy to process and have been widely used in the last century. However, due to the special interlayer structure of graphite anodes, fluorine gas is prone to chemical reaction with the graphite layers, forming a passivation layer, which causes a sharp drop in current and makes the electrolysis process impossible.[6,7] Amorphous carbon materials do not possess the layered structure of graphite, and the depth of fluorine entering its surface is much less than that of graphite electrodes, thus it is difficult to form an interlayer structure, which can weaken the "anodic effect".[8–10] Furthermore, amorphous carbon plates still cannot operate under high current density for a long time. Carbon plates meet the industry standards, namely, their density is 1.7 g cm^{-3}, resistivity is 38 μΩ m, and resistance to pressure is 70 MPa. However, those that meet the standard do not have the longest life, which indicates that the standard set by the industry specification can no longer be used for the evaluation of carbon plates. One strategy to solve this problem is the use of porous carbon plates, in which bubbles can be discharged rapidly from their pores. However, porous carbon plates can be easily broken, and it is difficult to achieve a good mechanical connection between the carbon plate and guide rod.[11] Another approach is to use a low permeability carbon plate and a lithium salt to increase the wettability.[12,13] This method not only speeds up the wetting of the fluorine gas, but also reduces the fracture of the carbon plates.

The volume density of carbon plates is closely related to their porosity, resistivity, thermal conductivity and mechanical

[a]*Chemical Science and Engineering College, Sichuan University, Chengdu 610065, PR China. E-mail: 18980632893@163.com; Tel: +862885405201*

[b]*Engineering Research Center of Comprehensive Utilization and Clean Processing of Phosphorus, Chengdu 610065, PR China*

properties, where the most effective way to prepare low permeability carbon plates is to increase their volume density.[14,15] According to the literature, it is difficult to improve the quality of the anode by increasing the actual density of calcined petroleum coke, but it is feasible to improve the adhesion and carbonization capacity of asphalt.[16,17] Presently, there are two main methods for the preparation of anodes, vibration forming and moulding. Although their principles are different, it is difficult to improve the existing technology due to the limitations of the slurry and methods employed.[18,19] In the 1980s, Union Carbide used a new method to produce blast furnace carbon bricks.[20] In this method, the molding and baking of carbon bricks are completed in one step. Carbon bricks have the characteristics of high density, low porosity and permeability, high thermal conductivity, and excellent mechanical properties. Cong[21] prepared a graphite anode with a density of 1.71 g cm^{-3} and resistivity of 49.5 μΩ m. Although the high temperature pressing method can improve the volume density of carbon plates, it still has some problems such as high energy consumption and limited industrialization.[22]

In this study, considering the existing problems such as anode effect, pulverization and fracture of the carbon plates of medium-temperature electrolytic cells, their mechanical properties, conductivity and corrosion resistance were improved by increasing their density. Compared with the carbon plate prepared by *via* traditional method, the life of our carbon plate increased by 40%. In this work, the current was directly passed into the carbon plate and its resistance was used for uniform heating to improve the density of the raw material, and then the volume density was further improved in the anode after impregnation with asphalt. Finally, the reason for the improvement in service life was analyzed by comparing the performance of the self-made carbon plate with that of an industrial carbon plate before and after electrolysis. The microstructure of the laboratory and factory carbon plates was observed *via* emission electron microscopy (FESEM). The graphitization degree of the carbon plates was analyzed *via* X-ray diffraction (XRD) and laser Raman spectroscopy (RM). Thermogravimetric differential thermal analysis (TG-DSC) was used to classify the carbon plates. A universal testing machine and conductivity test were employed to test the compressive properties of the samples before and after their use. The analysis and practical application showed that the high-performance carbon plates exhibited a prolonged life, allowing the stable production of fluorine gas.

2 Materials and methods

2.1 Materials

Petroleum coke was supplied by Shanghai YouYi Metallurgical Material Co., LTD. (China). Modified pitch was supplied by Shanghai Baosteel Chemical Co., LTD. (China). Details of the main components of the petroleum and modified pitch are shown in Tables 1 and 2, respectively.

Coke was graded according to the required particle size, and fine coke was obtained by ball grinding.

Table 1 Petroleum coke micro-element composition

Microelement	Fixed carbon	Ash	Volatile	Moisture	S
Content (%)	98.5	0.5	0.5	0.5	0.2

Table 3 shows the size distribution of the coke particles used for making the anode paste. The pitch/coke ratio was 16.5/100 for all the samples.

Sample preparation. Petroleum coke was mixed with bitumen ranging from small to large in size. A mixer was used to mix them for 25 min at 170 °C, and the obtained paste was pressed in high-pressing molds to form cylinders with dimensions of 300 × 600 × 70 mm. The mold temperature was 120–240 °C and the suppression time was 30 min. Under the protection of a nitrogen atmosphere, the samples were heated using a program and kept at 1250 °C for 96 h. Then the roasted carbon plates were impregnated with asphalt and roasted again. The specific experimental steps are shown in Fig. 1.

2.2 Carbon plate electrolysis experiment

The experiment was performed at the China National Nuclear 272 Uranium Industry Co. LTD. Medium-temperature electrolysis was based on a KF : HF ratio of 1.8 : 2 as the electrolyte and AHF as the raw material for electrolysis using a direct current of 0–10 kA. During the electrolysis process, the positive grid voltage was 5.5–8.0 V and the negative grid voltage was 2.5–4.0 V during normal operation. If the positive grid voltage exceeded 8 V, this indicated that the carbon plate was polarized, and the carbon plate needed to be pressurized. The performance test was preformed using the self-made carbon plate and commercial carbon plate from Jilin Carbon Co., LTD. The size of the carbon plate sheet was 300 × 600 × 70 mm, and the electrolytic cell contained 24 carbon plates. In this work, the self-made carbon plate (a) and Jilin carbon plate (b) were employed for comparative experiments, and the operating parameters and operating time were recorded. Finally, a resistivity test is conducted to determine the thickness of the passivation layer, and a compressive test was conducted to determine the corrosion resistance of the carbon plates. The specific experimental steps are shown in Fig. 2.

2.3 Characterization of carbon plate

The internal morphology of the sample was observed *via* field emission electron microscopy (SEM, VGEA3-SBH), and the degree of graphitization was measured *via* laser Raman spectroscopy and XRD (Empyrean, PANalytical) with CuKα radiation (λ = 1.5406 Å). Thermogravimetric-differential scanning calorimetry (TG-DSC, STA 449F3) was employed to analyze the

Table 2 Properties of modified coal bitumen

Softening point (°C)	108.50
β-Resin insoluble (%)	21.27
Moisture (%)	4.07
Ash content (%)	0.32
Coke value (%)	56.70
Quinoline insoluble (%)	7.20

Table 3 Size distribution of coke particles in the paste samples

Size range (mm)	0.787–0.60	0.3–0.075	0.075–0.0374	<0.0374
Wt%	12	23	40	25

thermal stability of the samples. A four-probe tester (KDB-1) was employed for the analysis of the resistance of the carbon plate before and after use. The compressive properties before and after use were tested using a universal testing machine (INSTRON). The viscosity of the asphalt at different temperatures was measured using a digital viscometer (DV-2).

3 Results and discussion

3.1 The effect of high-temperature mould pressing on bulk density

Pressing was a key step in the preparation of the green carbon anode, which directly affects the performance of roasted samples. The main factors affecting pressing are the forming pressure and temperature, where the bulk density of the green carbon anode varies with high-temperature mould pressing, as shown in Fig. 3. According to Fig. 3, the bulk density of the green carbon anode in the first stage (120 °C–200 °C) increased rapidly with an increase in temperature, and this is when the asphalt changed from the solid to liquid state. The mold transmitted potential energy to the material, causing the asphalt to be immersed in the aggregate microholes, and with an increase in pressure, the tighter the solid particle contact, the lower the porosity. In the second stage (200–240 °C), the bulk density of the green carbon anode decreased, which may be due to the decrease in viscosity and increase in fluidity with a further increase in temperature, leading to wall flow or groove flow. In addition, with a gradual increase in pressure, particle deformation and friction between the paste and mold, a vertical external force was applied to the material layer, which affected the dispersion of the powder among the particles and caused the density formed by the green carbon anode to exhibit an uneven distribution, while the volume density decreased. It was found that the density of the green carbon anode increased with an increase in pressure. Due to the irregular surface of the particles, an arch bridge effect was formed between them. In the process of pressure forming, the arch bridge effect was destroyed, and the pores between the particles were filled, and their positions

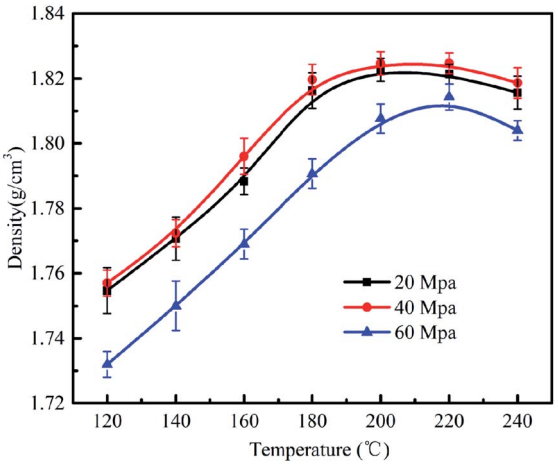

Fig. 3 Effect of pressure and temperature on the density of the green carbon anode.

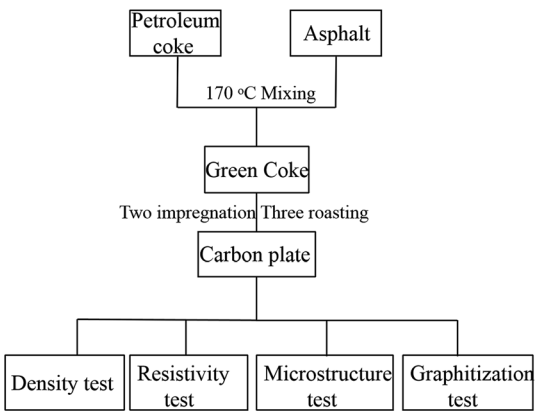

Fig. 1 Schematic of the experimental procedure.

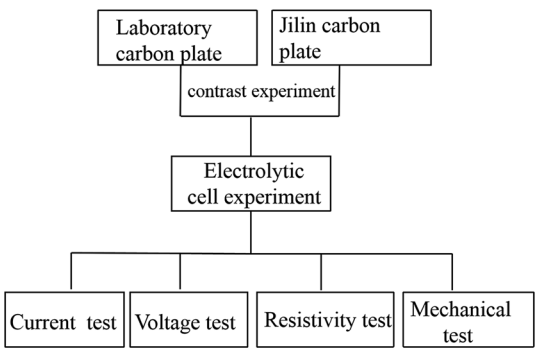

Fig. 2 Flow chart for the performance test.

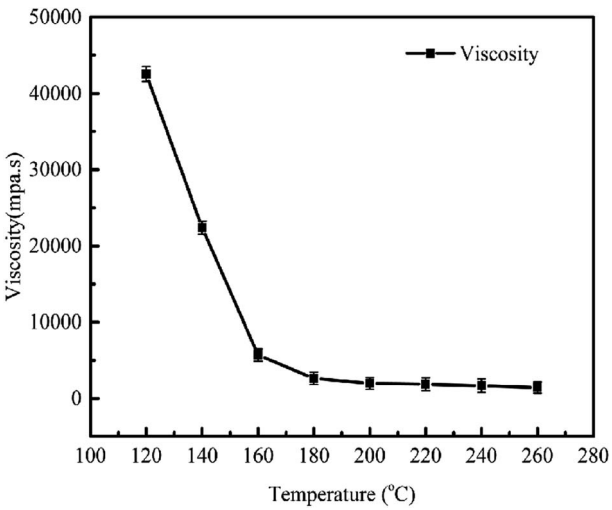

Fig. 4 Change in the viscosity of asphalt at different temperatures.

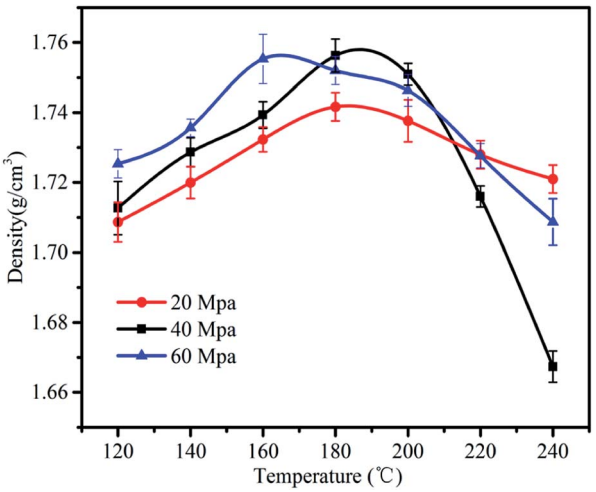

Fig. 5 Density of the green carbon anodes and prebaked anodes at different molding temperatures.

rearranged. With an increase in the external pressure, the particles deformed, and the contact form changed from the initial point contact to surface contact,[23] the number of contact between particles increased, the distance shortened and the contact surface increased.[24] The formulation was formed by mixing petroleum coke with different grain sizes, and in order to determine the appropriate forming pressure, pressure of 20 MPa and 40 MPa were applied. Consequently, the volume density of the raw material decreases with an increase in pressure, the contact distance between particles gradually decreased, and the pores became smaller; therefore, the volume density has a positive correlation. When the pressure increased to 60 MPa, the point contact changed to surface contact between particles, and the excessive pressure may have led to the destruction of the structure of the large particles, which reduced the probability of surface contact between particles and increased the pore spacing, thus leading to a decrease in the volume density of the raw material instead.

3.2 The effect of pressure and temperature on volume density after roasting

The viscosity of the asphalt decreased with an increase in temperature. As shown in Fig. 4, at 140–180 °C, due to the high viscosity and poor fluidity of the asphalt, it covered the surface of the petroleum coke particles, and only a small amount of asphalt entered the pores of the petroleum coke under the effect of applied pressure. Thus, this stage is called "cold molding".[25,26] When the external pressure disappears, the low forming temperature cannot eliminate the residual stress. In the roasting process, when the temperature exceeded the softening point, the residual stress in the sample was slowly released, leading to its volume expansion. With an increase in pressure, more asphalt entered the pores of the petroleum coke, and the residual stress decreased. Specifically, with an increase in pressure, the volume expansion decreased and the density increased. At 180–240 °C, the asphalt had a lower viscosity, and thus a larger amount of asphalt entered the pores of the petroleum coke, resulting in more compact contact between the particles, which is called "high-pressing mould".[27] Accordingly, the surface of the particles was coated with less asphalt and not influenced by residual stress. With an increase in pressure, the contact time between the particles gradually increased, the distance shortened, and the internal pores decreased. In the roasting process, the volatiles produced by the asphalt were not sufficiently discharged, and thus accumulated in the interior, which led to an increase in internal pressure and the expansion of volume density, thus leading to an increase in pressure and decrease in volume density.

As shown in Fig. 5, the green carbon anode was prepared *via* high temperature molding at 120–180 °C, and its density increased with an increase in temperature after roasting. At a pressure of 40 MPa and temperature of 180 °C, the carbon plate density was 1.74 g cm^{-3}, while the industry index is 1.70 g cm^{-3}. The density of the carbon blocks prepared in this experiment increased by 0.04 g cm^{-3}, indicating that the high-pressing molding method is beneficial for the improvement of their bulk density.

The density decreased in the temperature range of 180–240 °C, and the reasons for this were analyzed by recording the changes in the weight and volume of the sample. Table 4 presents the volume and weight changes at different temperatures at a pressure of 40 MPa. As shown in Table 4, the decrease in the volume density of the roasted samples is mainly due to the release of a large amount of volatiles from the asphalt. Simultaneously, with an increase in the pressing temperature in the range of 200–240 °C, the accumulation of grains on the surface of the raw embryo became more compact and the porosity decreased. In the roasting process, when the air and

Table 4 The change rate of the volume and weight of the prebaked anodes at different molding temperatures

Temperature (°C)	First baked weight change $(m_1 - m_0)/m_0$	First baked volume change $(v_1 - v_0)/v_0$	Rate of density change (ρ_1/ρ_0)
120	−(4.9001 ± 0.01)	−(0.0276 ± 0.01)	0.9760 ± 0.01
140	−(4.5022 ± 0.01)	−(0.0215 ± 0.01)	0.9762 ± 0.01
160	−(4.0302 ± 0.01)	−(0.0156 ± 0.01)	0.9753 ± 0.01
180	−(4.1003 ± 0.01)	−(0.9562 ± 0.01)	0.9669 ± 0.01
200	−(3.9302 ± 0.01)	0.5330 ± 0.01	0.9696 ± 0.01
220	−(4.3302 ± 0.01)	1.5002 ± 0.01	0.9421 ± 0.01
240	−(3.9301 ± 0.01)	4.5701 ± 0.01	0.9204 ± 0.01

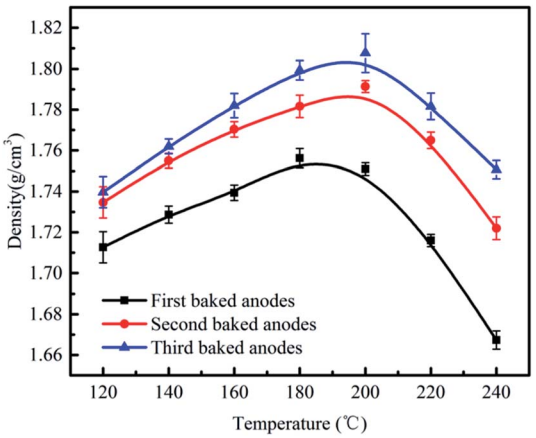

Fig. 6 Variation in the density upon subsequent treatment at different molding temperatures.

asphalt mixed in the molding process decompose at high temperature, the volatiles do not have sufficient time to be discharged and accumulate in the interior, resulting in an increase in internal pressure and volume expansion.

3.3 Bitumen impregnation process

The density of the carbon plate is an important index, which is closely related to voidage, resistivity, corrosion, resistance and mechanical properties. Therefore, increasing the bulk density of the anode can prolong its service life, reduce the influence of manual operation, and ensure the reliable and stable operation of the electrolytic cell.[12] During the baking of the green carbon anode, the release of a large amount of volatiles in the asphalt les to an increase in the amount of pores in the carbon plates, and a further decrease in volume density under the influence of the "air pressure model".[13] The density of the prebaked anode was further increased by pressurizing the asphalt into an anode and then roasting it. Carbon plates were placed in bitumen at 200 °C under atmospheric pressure for 8 h and then roasted twice. As shown in Fig. 6, at a temperature of 180 °C and a pressure of 40 MPa, the density of the carbon plates was 1.816 g cm^{-3}, which increased by 0.076 g cm^{-3}. Thus, the asphalt impregnation roasting process revealed that the bulk density of the carbon plate can be improved effectively.

The weight and volume change rates of three samples were measured at each temperature of the carbon plates at different molding temperatures. The reason for the increase in density was determined by comparing the change in weight with the change in volume. As can be seen from the analysis in Table 5, the weight gain rate of the second roasting was 1.8–2.8, and the volume expansion in the second roasting was 0.13–1.01. The weight gain rate of the third roasting was 1.1–1.7, and the volume in the third roasting was 0.19–0.091. This indicates that the increase in density was mainly caused by the filling of the internal pores of the asphalt, and thus multiple pores on the surface of the carbon block effectively released the internal gas pressure and reduced the decrease in density caused by volume expansion.

3.4 Experiment on electrolysis of fluorine

3.4.1 Basic parameters of laboratory carbon plates and Jilin carbon plates. The preparation of the laboratory carbon plates involved the addition of petroleum coke ranging from small to large in size to bitumen. A mixer was used to mix them for 25 min at 170 °C, and the obtained paste was pressed in a high-pressing mold into cylinders with dimensions of 300 × 600 × 70 mm. The mold temperature was 180 °C, the forming pressure was 40 MPa, and the pressing time was 30 min. Under the protection of a nitrogen atmosphere, the samples were heated using a program and kept at 1250 °C for 96 h. Then the roasted carbon plates were impregnated with asphalt and roasted again. The performance of the carbon plates was tested and compared with that of carbon plates purchased from Jilin Carbon Co., LTD in the laboratory. The indicators of the carbon plates are shown in Table 6. The mixing of graphite in the fluorocarbon plate will lead to pulverization and seriously affect the electrolysis process.

The degree of graphitization of the fluorocarbon plate is shown in Fig. 6. The XRD tests showed that both the laboratory (Fig. 7a) and Jilin carbon plates (Fig. 7b) are amorphous carbon, corresponding to the reference standard for amorphous carbon (Fig. 7c) and graphite (Fig. 7d) (amorphous carbon: JCPDS Card No. 26-1080, and graphite: JCPDS Card No. 41-1487). The Raman tests showed that the laboratory carbon plates (Fig. 7e) had $I_D/I_G = 1.1189$ and Jilin carbon plates (Fig. 7f) $I_D/I_G = 1.082$, both indicating that there was no graphite in both of them.

Table 5 Weight and volume changes of the anodes after subsequent treatment at different temperatures

Temperature (°C)	Second baked weight change $(m_2 - m_1)/m_1$	Second baked volume change $(v_2 - v_1)/v_1$	Rate of density change (ρ_2/ρ_1)	Third baked weight change $(m_3 - m_2)/m_2$	Third baked volume change $(v_3 - v_2)/v_2$	Rate of density change (ρ_3/ρ_2)
120	1.8104 ± 0.01	0.5231 ± 0.01	1.0128 ± 0.01	1.1996 ± 0.01	0.9091 ± 0.01	1.0028 ± 0.01
140	1.8001 ± 0.01	0.2833 ± 0.01	1.0152 ± 0.01	1.0993 ± 0.01	0.7072 ± 0.01	1.0039 ± 0.01
160	2.8002 ± 0.01	1.0101 ± 0.01	1.078 ± 0.01	1.6001 ± 0.01	0.8931 ± 0.01	1.0073 ± 0.01
180	2.0201 ± 0.01	0.9561 ± 0.01	1.0106 ± 0.01	1.2002 ± 0.01	0.4960 ± 0.01	1.0101 ± 0.01
200	2.6812 ± 0.01	0.3760 ± 0.01	1.0231 ± 0.01	1.7012 ± 0.01	0.4942 ± 0.01	1.0124 ± 0.01
220	2.4303 ± 0.01	0.1311 ± 0.01	1.0241 ± 0.01	1.5001 ± 0.01	0.197 ± 0.01	1.0130 ± 0.01
240	2.8402 ± 0.01	0.2350 ± 0.01	1.0267 ± 0.01	1.5503 ± 0.01	0.2463 ± 0.01	1.0163 ± 0.01

Table 6 Basic parameters of (a) laboratory carbon plate and (b) Jilin carbon plate

Test item	Sample 1 (a)	Sample 2 (b)	Test method
Bulk density (g cm^{-3})	1.81 ± 0.10	1.73 ± 0.12	YS/T63.7-2006
Compression strength (MPa)	95.0 ± 4.50	77.50 ± 17.50	YS/T63.15-2012
Total porosity (%)	11.0 ± 2.00	15.60 ± 1.50	YS/T63.7-2006
Degree of graphitization (%)	0.00	0.00	YS/T73.3-2010
Ash content (%)	0.44 ± 0.10	0.42 ± 0.08	YS/T63.19-2012
Electrical resistivity (μΩ m)	25.80 ± 2.50	36.70 ± 1.30	YS/T63.2-2006

Fig. 8 displays the SEM images comparing the micromorphology of the industrial and laboratory carbon anodes. According to Fig. 8b, the comparison shows that the industrial carbon anode has a lamellar structure and its particles are relatively dispersed. The structure of the laboratory carbon anode in is relatively compact and disrupted (Fig. 8a). The increase in density is due to the decrease in the grain spacing and the change of the atomic structure in the grains with an increase in temperature through high-press moulding, which effectively reduced the porosity and defects in the samples.

In addition, by impregnating and baking the bitumen, the adhesion between the particles was further strengthened, thus filling the gaps. YS/T 63.2-2006 was used to test the resistivity of the laboratory carbon anode, which was determined to be 25.8 μΩ m, less than the standard of 40 μΩ m for the industrial carbon anode. This also indicates that the high-temperature

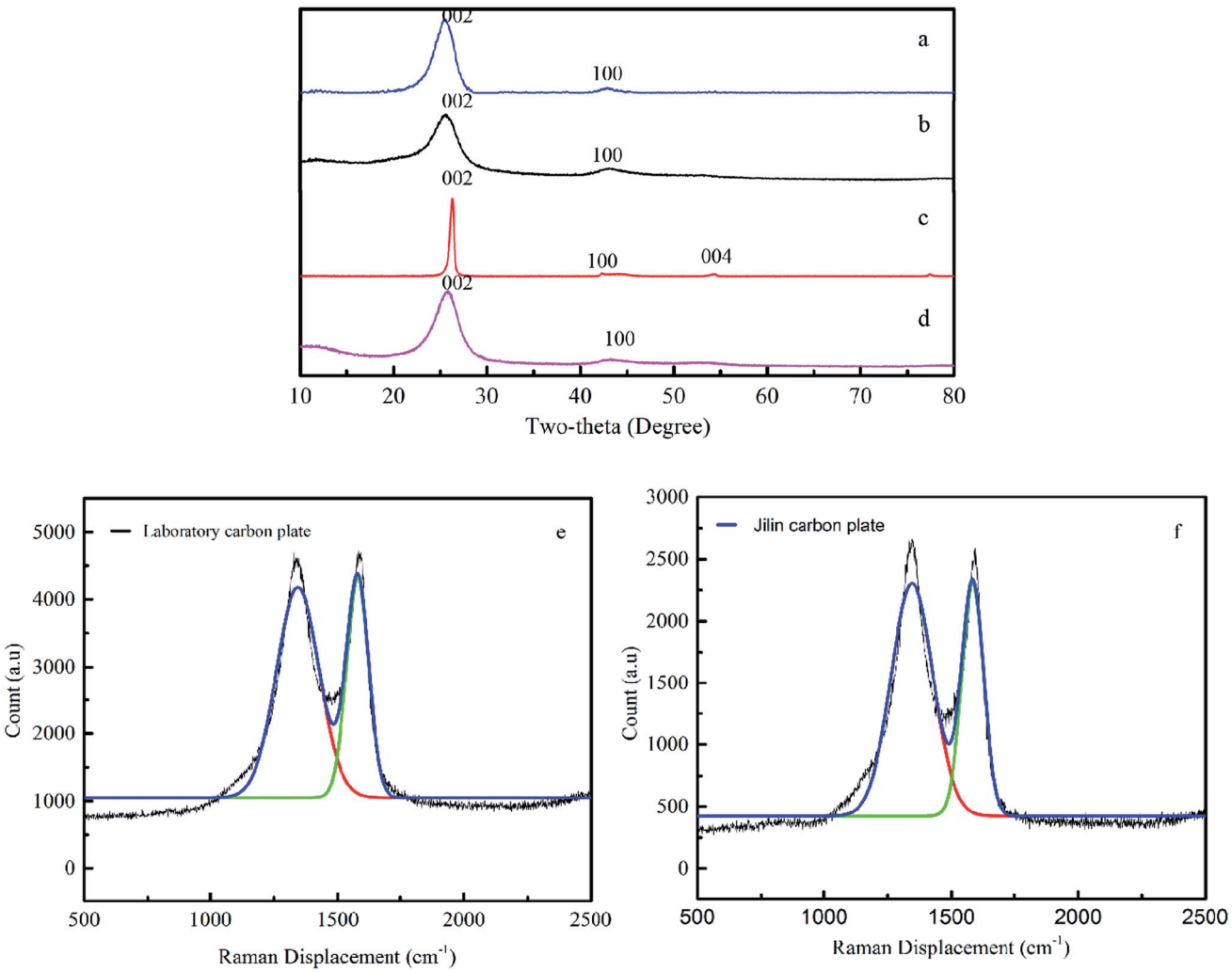

Fig. 7 XRD patterns of (a) laboratory and (b) Jilin carbon plates, (c) graphite sample and (d) petroleum coke raw material. Raman spectra of (e) laboratory and (f) Jilin carbon plates.

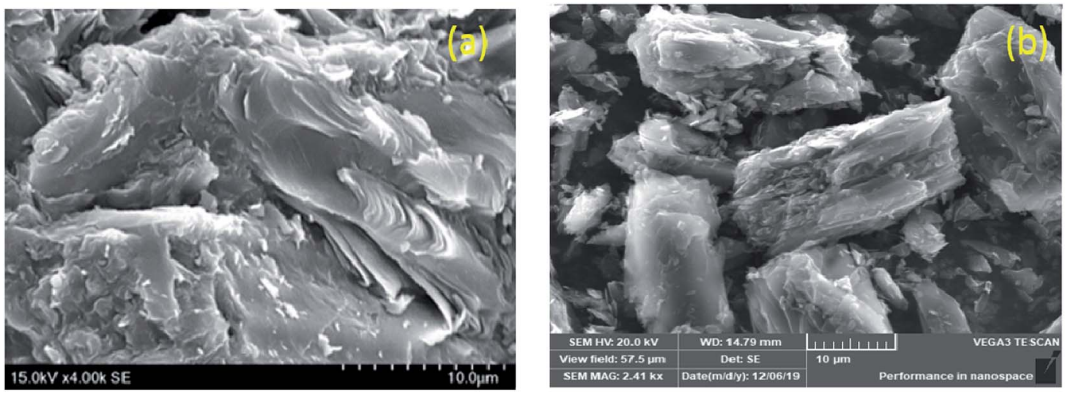

Fig. 8 SEM images of (a) laboratory carbon anode and (b) Jilin carbon anode.

mould pressing method can promote the association of ionic groups in the amorphous carbon structure of coke, increase the number of conductive ions, and reduce the resistivity, while increasing the density.

3.4.2 Classification of the carbon plates by thermal analysis. The analysis of the carbon materials for used as anodes in the production of fluorine was carried out using the methods reported by Sofronov, V. L[28] for carbon plate classification. The sample was heated to 900 °C in an air atmosphere at a rate of 10 °C min^{-1}. The result of the differential thermal decomposition is shown in Fig. 9. The oxidation rate was as follows:

ΔA (%) – the sample mass decreased before the derivative of the DSC curve reached its maximum value.

ΔB (%) – the ratio of the DSC extremum to the derivative strength of the two extremums (at 650–800 °C intervals).

ΔT (°C) – the temperature difference between the first and second extreme values in the DSC derivative.

The carbon plates were classified according to the following criteria:

(1) Quality grade 1: ΔA = 50–55%; B = 0%; ΔT reach 40 °C, and the number of extremes (n) = 1 and 2.

(2) Quality grade 2: ΔA = 56–65%; B = 51–56%; ΔT = 41–60 °C, and the number of extremes (n) = 2.

(3) Quality grade 3: ΔA = 66–70%; B = 57–60%; ΔT = 61–70 °C, and the number of extremes (n) = 3.

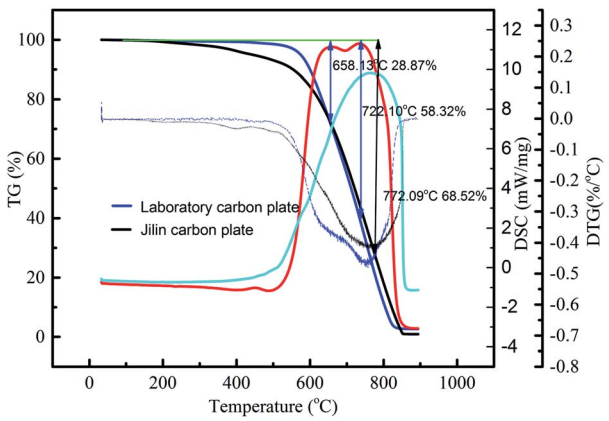

Fig. 9 Classification of the different grades of carbon plates.

(4) Quality grade 4: ΔA = 70%; B = 61–70%; ΔT = 71–80 °C, and the number of extremes (n) = 4.

There are two small peaks in the carbon plate pyrolysis rate DSC curve, and the DTG curve also fluctuates in the corresponding position, indicating that substances with different reaction rates reacted. The above analysis is based on the Raman test of the laboratory carbon plate (Fig. 7e) and Jilin carbon plate (Fig. 7f), which proves that the graphitization degree of the laboratory carbon plate is less than that of the Jilin carbon plate. Perhaps the first peak of the laboratory carbon plate in the DSC curve is the oxidation of the indefinite carbon. The second peak occurs at higher temperatures, which is possibly due to the transformation of a small amount of indefinite carbon into an ordered layered structure, leading to oxidation reactions requiring higher activation energies.[29]

As shown in Table 7, the maximum weight loss of the laboratory carbon plates is 58.32% and that of the Jilin carbon plate is 68.52%. This indicates that the laboratory carbon plate is more compact and has a better oxidation performance.

3.5 Operation comparison of laboratory and industrial carbon plates

The test site was the China Nuclear 272 Uranium Industry Co., LTD. The laboratory and Jilin carbon plates were put into electrolytic cell No. 3 (Fig. 10b) and No. 25 (Fig. 11d), respectively, and the electrolytic fluorine preparation experiment was carried out in accordance with the factory technical manual. The current, positive grid voltage, negative grid voltage and operating days of the carbon plate in the electrolysis process were recorded. Fig. 10a shows a bar chart of the operating days as a function of current for the laboratory carbon plates, and Fig. 11a shows the same for the Jilin carbon plate. As shown in Fig. 10a and 11a, the laboratory carbon plates ran for 61 days longer than the Jilin carbon plates, respectively, and its current operation was relatively stable, indicating that the high-density carbon plate can operate more stably under electrolytic conditions. As shown in Table 8, the voltage of the Jilin carbon plate was higher than that of the laboratory carbon plate, which may be due to the non-conductive passivation layer formed by fluorine gas inside the carbon plate, which intensifies the retention

Table 7 Differential thermal decomposition of the different carbon plates

Sample	ΔA (wt%)	ΔB (%)	ΔT (°C)	Quality grade
Laboratory carbon plate	28.87, 58.32	29.45	63.97	II
Jilin carbon plate	68.52	0.00	0.00	III

of bubbles on the positive plate and increases the resistance between the anode and cathode, thus increasing the voltage between the electrodes at the same input current. By contrast, the anode voltage of the laboratory carbon plate was in a stable state, which indicates that the carbon plate is in a stable state in the electrolysis process and can better resist the occurrence of the "anode effect".

3.6 Analysis of laboratory and factory carbon decanting

The passivation layer is formed because of the long-term contact between fluorine gas and the anode material. This fluorinated film not only increases the electric potential of the anode, but more seriously reduces the wettability of the electrolyte on the anode surface and effective area of the carbon plate, making it impossible for electrolysis to continue. The industrial method to eliminate the passivation layer is to remove it by adding high pressure to make the surface burn. However, multiple cycles may lead to a decline in the strength of the carbon plate, leading to fracture. Amorphous carbon does not possess a layered structure like graphite, and thus cannot form a thick passivation layer. Therefore, in the infrared test, the F–C bond peak strength was low and the formation of a passivation layer could not be judged intuitively. Thus, the carbon plate was sliced, and the positions at different depths

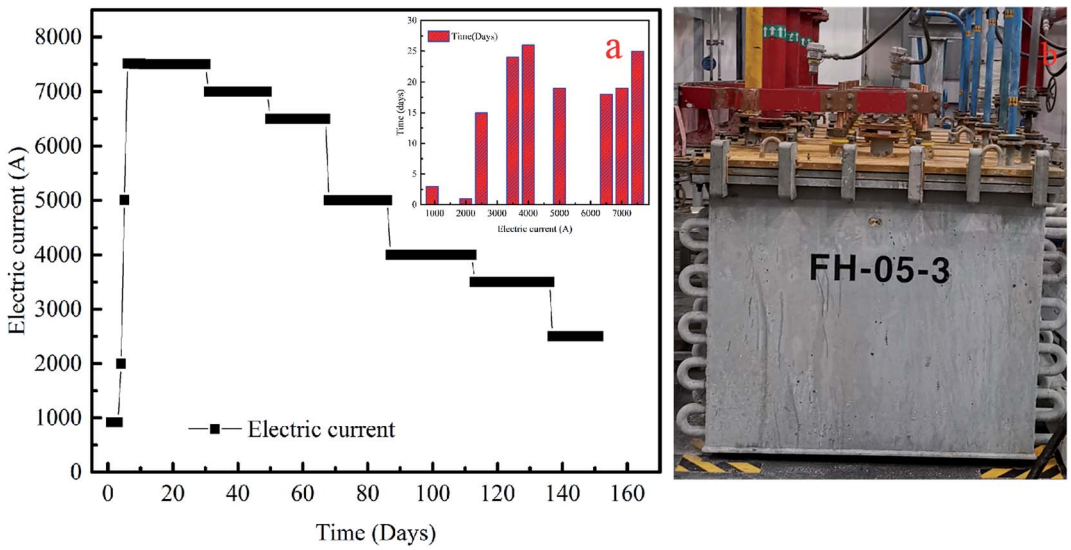

Fig. 10 Operating data of (a) laboratory carbon plate and (b) carbon plate operating unit.

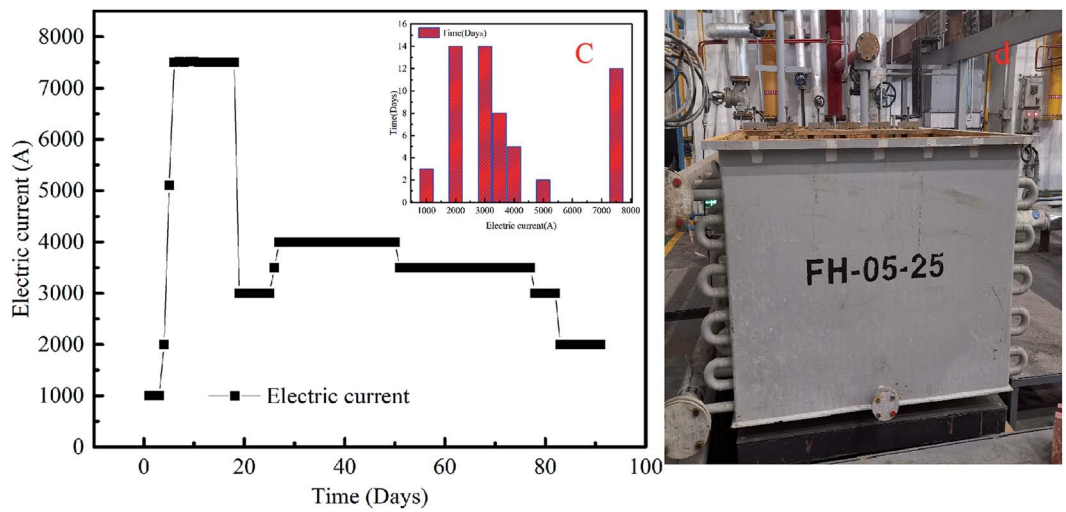

Fig. 11 Operating data of (a) Jilin carbon plates and (b) carbon plate operating unit.

Table 8 Comparison of the basic operation data for the different carbon plates

Maximum running current (A)	Minimum operating current (A)	Positive voltage range (V)	Negative voltage range (V)	Number of days run	Note
7500	2000	6.87–8.31	3.06–3.16	90	Jilin carbon plate
7500	2000	5.80–6.60	2.60–3.80	151	Laboratory carbon plate

inside the carbon plate were tested with a four-probe resistivity tester.

As shown in Table 9, the resistance on the surface of the Jilin carbon plate and the laboratory carbon plate increased to a large extent, indicating that a passivation layer was formed on both surfaces, which may be greater on the Jilin carbon plate than that on the laboratory carbon plate. Based on the overall comparison, the resistivity of the laboratory carbon plate was basically stable at a depth of 5 mm, while that of Jilin carbon plate was basically stable at a depth of 7.5 mm. This indicates that the high density carbon plate may obstruct the maturation rate of fluorine gas in the internal reaction, thus ensuring the long-term stable operation of electrolysis.

Table 9 Resistivity of the carbon plate at different depths

	Resistivity test (μΩ m)	
Sample thickness (mm)	Laboratory carbon plate	Jilin carbon plate
70.00 ± 1.12	133.78 ± 7.90	186.70 ± 5.80
67.50 ± 0.38	70.08 ± 2.60	165.80 ± 3.18
65.00 ± 0.47	44.76 ± 4.40	85.41 ± 4.23
62.50 ± 0.36	36.15 ± 5.38	57.03 ± 2.88
60.00 ± 0.58	33.51 ± 4.08	55.87 ± 4.80

3.7 Compressive strength test of carbon plates before and after electrolysis

The "anode effect" is inevitable in the electrolytic process on the carbon plate, which needs to be solved by adding a high-pressure combustion passivation layer or grinding method, which may lead to the fracture of the carbon plate and require the full replacement of the carbon plate. Therefore, the stability of the mechanical properties of the carbon plate is an important index. As shown in Fig. 12, the surface of the laboratory carbon

Fig. 12 Changes in the laboratory carbon plate and Jilin carbon plate before (a and c) and after (c and d) electrolysis, respectively.

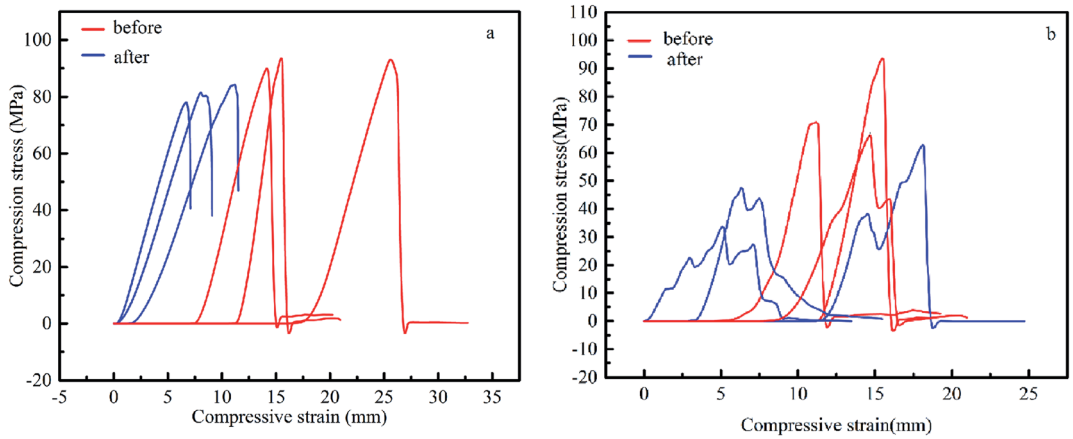

Fig. 13 Comparison of the compressive tests for the (a) laboratory carbon plate and (b) Jilin carbon plate.

plate had no obvious change before and after electrolysis, which indicates that its corrosion resistance was strong. The morphology of the Jilin carbon plates changed obviously after electrolysis, and most of them were broken after the electrolysis test, indicating that the mechanical properties of low-density carbon plates are poor and cannot resist thermal shock.

The compression test was conducted by sampling three different locations of the carbon plates and preparing a cylinder with a diameter of 50.0 mm ± 0.4 mm, height of 50 mm ± 0.1 mm, and parallelism of ±0.05 mm between the two surfaces. Then the sample was subjected to a continuous, non-impact load at a rate of 0.5 N mm^{-2} per second until it was destroyed. The compressive test data were randomly selected from different positions of the carbon plates for sampling. The same series of samples in the figure differ because the mechanical strength of the carbon material was determined by its matrix strength and porosity.[30] The carbon plates were composed of petroleum coke with different particle sizes, which may result in an uneven particle size and pore distribution. It can be seen from Fig. 12 that the compressive strength of the laboratory carbon plates before electrolysis was 95.0 ± 4.5 MPa. This indicates that the ratio and distribution of the different petroleum coke particle sizes in the laboratory carbon plates were more reasonable compared with that of the Jilin carbon plate, where its compressive strength was between 77.5 ± 17.5 MPa, and the ratio of the different particle sizes is unreasonable and their distribution is uneven. This led to a great difference in compressive strength before electrolysis. As shown in Fig. 13a, the compressive properties of the laboratory carbon plate changed slightly after electrolysis, indicating that its internal structure was still stable. In contrast, the Jilin carbon plate (Fig. 13b) exhibited great changes in its mechanical properties before and after electrolysis, especially after the electrolytic sample load reached the limit, in the form of a "wave", characterized by a false body fracture. This may be because the sample density was low, and under the condition of further electrolytic internal ablation, the load was emptied, and the holes became the main source of fracture. Thus, the comparison of the mechanical properties before and after electrolysis showed that the high density carbon plate has a more stable corrosion resistance.

4 Conclusion

(1) Adopting a standard module carbon plate size molding method and asphalt immersion process not only reduced the roasting cost, but the density and resistivity of the carbon plate reached 1.81 g cm^{-3} and 25.8 μΩ m by high temperature mould pressing and impregnation. Compared with the industrial plate, the carbon density increased by 4.5% and the resistivity decreased by 29.7%.

(2) The operating days of the laboratory carbon plates were 67.7% more than that of the Jilin carbon plates, and the current did not fluctuate greatly, indicating that the laboratory carbon plates have better corrosion resistance and polarization resistance.

Conflicts of interest

The authors declare that they have no known competing financial interests or personal relationships that could have appeared to influence the work reported in this paper.

Acknowledgements

This study is financially supported by the National key research and development plan: Electrochemical preparation technology of high value-added fine chemicals (Project No.: 2017YFB0307504). We sincerely acknowledge the experiment site support of China National Nuclear 272 Uranium Industry Co. LTD.

References

1 A. J. Rudge, *Industrial electrochemical processes*, Elsevier Publishing Company, 1971, pp. 1–69, DOI: 10.1002/elan.201000421.

2 P. L. Crouse, Fluorine: a key enabling element in the nuclear fuel cycle, *J. South. Afr. Inst. Min. Metall.*, 2015, **115**, 931–935, DOI: 10.17159/2411-9717/2015/v115n10a5.

3 G. Camozzo and S. Pizzini, Study on some fluorination techniques. Description of a plant for the production of fluorine and fluorine halides halides, *Energ. Nucl.*, 1960, **7**, 145–152.

4 L. Bai and B. E. Conway, Electrochemistry of anodic fluorine gas evolution at carbon electrodes: part III characterization of activated carbon anodes following onset of the 'anode effect, *J. Fluorine Chem.*, 1990, **20**, 925–931, DOI: 10.1007/bf01019567.

5 A. Tasaka, K. Miki, T. Ohashi, S. Yamagushi, M. Iwanaga and J. Aritsuka, *J. Electrochem. Soc.*, 1994, **14**, 11460, DOI: 10.1002/chin.199441015.

6 H. Imoto and N. Watanabe, A study on the anode effect in KF-2HF system. II. Difference in anodic behavior between edge plane and layer-plane of pyrolytic graphite, *Bull. Chem. Soc. Jpn.*, 1976, **49**, 1736–1739, DOI: 1736-173910.1246/bcsj.49.1736.

7 H. Imoto, T. Nakajima and N. Watanabe, ChemInform abstract: a study on anode effect in KF-2HF system part 1, ESCA spectra of carbon of carbon and graphite anode surfaces, *Chem. Informationsdienst*, 1975, **6**, 11–14, DOI: 10.1002/chin.197531012.

8 L. Bai and B. E. Conway, Electrochemistry of anodic fluorine gas evolution at carbon electrodes: part III characterization of activated carbon anodes following onset of the anode effect, *J. Appl. Electrochem.*, 1990, **20**, 925–931, DOI: 10.1007/bf01019567.

9 V. Gupta, T. Nakajima, Y. S. M. Ohzawa and B. Zemva, A study on the formation mechanism of graphite fluorides by Raman spectroscopy, *J. Fluorine Chem.*, 2003, **120**, 143–150, DOI: 10.1016/S0022-1139(02)00323-8.

10 H. Groult, Electrochemistry of fluorine production, *J. Fluorine Chem.*, 2003, **119**, 173–189, DOI: 10.1016/S0022-1139(02)00252-X.

11 A. J. Allen and A. J. Bard, *Encyclopedia of electrochemistry of the elements*, Dekker, New York, N.Y., 1976, vol. VII, DOI: 10.1149/1.2134237.

12 R. M. Reeves, *J. Electroanal. Chem. Interfacial Electrochem.*, 1978, **91**, 299–300, DOI: 10.1016/S0022-0728(78)80110-7.

13 A. A. Vlasov, V. M. Sizyakov, D. A. Seregin, M. V. Molin and R. N. Idiyatulin, Reducing the incidence of anode effects at the Krasnoyarsk aluminum plant, *Metallurgist*, 2011, **55**, 601–606, DOI: 10.1007/s11015-011-9474-7.

14 C. C. Shen, *Chemistry and technology of uranium and its compounds*, Atomic Energy Press, 1991.

15 S. L. Ye, J. Xiao, J. H. Yang, Y. Q. Lai, Z. Zou and Y. X. Liu, Laboratory study of modified prebaked carbon anodes for aluminum electrolysis, *Chin. J. of Nonferrous Met.*, 2003, **13**, 245–249, DOI: 10.19476/j.ysxb.1004.0609.2 003.01.045.

16 Z. Kuang, J. Thonstad, S. Rolseth and M. Sørlie, Effect of baking temperature and anode current density on anode carbon consumption, *Metall. Mater. Trans. B*, 1996, **27**, 177–183, DOI: 10.1007/BF02915043.

17 F. Q. Liu, Y. X. Liu, U. Mannweiler and R. Perruchond, Effect of coke properties and its blending recipe on performances of carbon anode for aluminium electrolysis, *J. Cent. South Univ. Technol.*, 2006, **13**, 647–652, DOI: 10.1007/s11771-006-0009-5.

18 S. H. Pan, S. J. Mi and L. W. Ding, Production of large scale cathode carbon block for aluminium by vibration molding, *Carbon Tech.*, 2010, **1**, 4–48.

19 J. V. Badding, High-pressure synthesis, characterization and tuning of solid state materials, *Annu. Rev. Mater. Sci.*, 1998, **281**, 631–658, DOI: 10.1146/annurev.matsci.28.1.631.

20 X. Jin, J. Li, S. L. Ye, Y. Q. Lai and Y. X. Liu, Laboratory study of property-modified prebaked carbon anode and application in large aluminum electrolysis cells, *J. Cent. South Univ. Technol.*, 2005, **129**, 68–71.

21 C. G. Cong and N. X. Feng, Study on resistance and thermal conductivity of semi-graphite carbon blocks roasted by electrothermal moulding, *Carbon Technol.*, 1995, **15**, 1–6.

22 Y. W. Wang, J. P. Peng, Y. Z. Di, Z. Yue and N. X. Nai, Production of carbon anodes by high-temperature mould pressing, *Trans. Nonferrous Met. Soc. China*, 2013, **23**, 3119–3124, DOI: 10.1016/S1003-6326(13)62842-3.

23 L. Yang, D. C. Nuai and X. G. Wu, Study on the preparation technology of tungsten–copper composite by hot pressing sintering, *J. Xihua Univ., Nat. Sci. Ed.*, 2005, **06**, 98–101, DOI: 10.18799/24131830/2019/4/202.

24 W. Z. Jiang, *Carbon technology*, Metallurgical Industry Press, Beijing, 2009, pp. 216–217.

25 M. Born, S. Starke and A. Seichter, Elastic behavior of electrode cokes and relaxation of press strains, *Carbon*, 1992, **30**, 141–145, DOI: 10.1016/0008-6223(92)90073-6.

26 M. Born, A. Seichter, S. Starke and B. Friberg, Characterization of baking behaviour of carbonaceous materials by dilatation investigations, *Carbon*, 1990, **28**, 281–285, DOI: 10.1016/0008-6223(90)90002-g.

27 M. Born, Pyrolysis and behaviour in the baking of industrial carbons, *Fuel*, 1974, **53**, 198–203, DOI: 10.1016/0016-2361(74)90011-8.

28 V. L. Sofronov, P. B. Molokov, A. V. Muslimova, A. V. Polyanskaya, Y. P. Damm and A. I. Rudnikov, Analysis of carbon materials used as anodes in fluorine production, *Bulletin of the Tomsk Polytechnic University Geo Assets Engineering*, 2019, **330**, 78–88, DOI: 10.18799/24131830/2019/4/202.

29 C. Z. Liu, W. M. Chen, M. C. Li, S. Hong, W. Z. Li, M. Z. Pan, Q. L. Wu and C. T. Mei, Rapid microwave activation of waste palm into hierarchical porous carbons for supercapacitors using biochars from different carbonization temperatures as catalysts, *RSC Adv.*, 2019, **9**, 19441–19449, DOI: 10.1039/C9RA03031J.

30 P. M. Wang, *Inorganic nonmetallic materials science*, Tongji University Press, Shanghai, 1999, pp. 38–41.